Study of ω-meson production in the reaction $pn \to d\omega$ at ANKE

S. Barsov, V. Koptev, S. Mikirtychiants
High Energy Physics Dept., Petersburg Nuclear Physics Institute, 188350 Gatchina, Russia

M. Hartmann, V. Hejny, A. Klingler, V. Leontyev, D. Oellers, H. Ohm, R. Schleichert, H. Ströher
Institut für Kernphysik, Forschungszentrum Jülich, D-52425 Jülich, Germany

A. Khoukaz
Institut für Kernphysik, Universität Münster, Wilhelm-Klemm-Str. 9, D-48149 Münster, Germany

S. Dymov, S. Merzliakov, V. Serdyuk
Lab. of Nuclear Problems, Joint Institute of Nuclear Research, 141980 Dubna, Russia

D. Chiladze, A. Kacharava, I. Keshelashvili
High Energy Physics Institute, Tbilisi State University 380186 Tbilisi, Georgia

S. Trusov
Institut für Kernphysik, Forschungszentrum Rossendorf

and the ANKE collaboration

6th April 2007

spokesmen:

S. Barsov, (barsov@pnpi.spb.ru)
and
R. Schleichert (r.schleichert@fz-juelich.de)

Contents

Abstract

We propose to measure total and differential cross sections of the $pn \to d\omega$ reaction from near threshold up to excess energies of Q=100 MeV by studying the reaction $pd \to p_{sp}d\omega$ on a deuterium target. The direct measurement of the low momentum spectator protons p_{sp} allows under the assumption of quasi-free kinematics the interpretation as the reaction $pn \to d\omega$ on a quasi-free neutron target. The $\sqrt{s}$ for this reaction is determined by knowing the beam momentum and measuring the spectator proton. The ω-meson is identified by the missing-mass technique.

The ANKE forward detection system provides the deuteron identification and momentum determination. Spectator proton identification, tracking and energy determination will be accomplished by the ANKE Silicon Tracking Telescopes. This setup allows to cover the full range of excess energies up to 100 MeV without changing the beam energy.
We plan to use the unpolarized proton beam of COSY and the D_2 cluster target for the ω production measurement.

1 Overview

Despite experimental studies of ω and ϕ meson production in nucleon-nucleon (NN) collisions near threshold have been started less than 10 years ago, the great progress was achieved by now. The pioneering data from the SPESIII ($pp \to pp\omega$) and the DISTO ($pp \to pp\phi$) collaborations have been significantly extended in a number of experiments carried out at COSY–TOF ($pp \to pp\omega$) and ANKE ($pp \to pp\omega/\phi, pn \to d\omega/\phi$). Being supported by extensive theoretical investigations performed the last decade, this study is aimed to obtain information on the production mechanism and its possible coupling to nucleon resonances which would shed a light on the short-range part of the NN interaction.

Another intriguing topic is to test the so-called Okubo–Zweig–Iizuka (OZI) rule [1] which is known to restrict the ϕ/ω production ratio to the value of $R_{OZI} \simeq 4.2 \cdot 10^{-3}$ [2]. A significant excess over this value may indicate an admixture of strange quarks to the nucleon wave–function. Though the experimental ϕ/ω production cross section ratio has been found to be much larger than R_{OZI} in several independent measurements, the production mechanisms of both mesons is required to be well established before this ratio may be unambiguously interpreted in terms of "hidden" strangeness.

Although the theoretical analysis of the whole set of data is still far from complete, recent calculations based on the effective meson–exchange theory show that ω–meson production is very sensitive to the interference of nucleonic and mesonic currents [20]. Due to the distinct isospin structures of the currents, their relative contributions may be effectively resolved using data on ω–meson production in both proton–proton and proton–neutron channels. It is interesting to note that even the existing low–statistics data on the $pn \to d\omega$ reaction were found to be helpful in order to achieve a better description of the $pp \to pp\omega$ data close to threshold without implicitly involving nucleon resonances which was necessary in earlier calculations [7]. However, it is clear that the accuracy of the existing data for ω–meson production in the pn isospin channel certainly is too low for the further development of theoretical models as well as for the determination of the ϕ/ω production ratio.

It is the aim of the present proposal to show that we can essentially decrease both the statistical and the systematic uncertainties of data for the pn $\to$ dω reaction using quasi-free production in a deuterium target and measuring the spectator proton in coincidence with the final state deuteron. As described below the use of two telescopes of large-size silicon detectors (STT) will allow us not only to increase the experimental acceptance but also to determine the angular differential cross section. Since the ω–meson production will be identified using the missing–mass technique, a large physical background is unavoidable. Despite the satisfactory description of the background by Monte–Carlo simulations has been achieved in previous experiment [12], in this proposal we used such simulations only for the estimation of the signal–to–background ratio. In fact, we plan to exploit an interpolation procedure using the kinematical transformation of the background missing mass distribution [4, 15].

In view of the results presented in this document, we request 2 weeks of beam-time to extract an energy dependence of total cross section for the Q-range of 20 to 100 MeV and to determine differential cross sections as well.

2 Physics case

2.1 Experimental Data and Theoretical Descriptions

Meson production in nucleon-nucleon (NN) collisions near threshold, where the number of partial waves involved in the process is significantly limited, is generally considered to provide important information on the NN interaction due to the relatively simple interpretation of data (see, for example, [3] and references therein). Therefore as soon as data on the production of isoscalar ω and ϕ mesons in proton–proton (pp) interactions near threshold became available [4–6] they were subject to extensive theoretical considerations [7–9] addressing the production mechanism and its possible coupling to nucleon resonances. Indeed, in line with the theoretical analysis of the $\pi^- p \to \omega n$ reaction [10, 11], K.Tsushima and K.Nakayama [7] have found that the energy dependence of the ω total cross section could not be satisfactory described without the inclusion of nucleon resonances. On the other hand, C.Fuchs *et al.* [8] have achieved a quite good agreement with all available data for ω total cross sections assuming that the production of this meson is strongly coupled to the $N^*(1535)$ resonance.

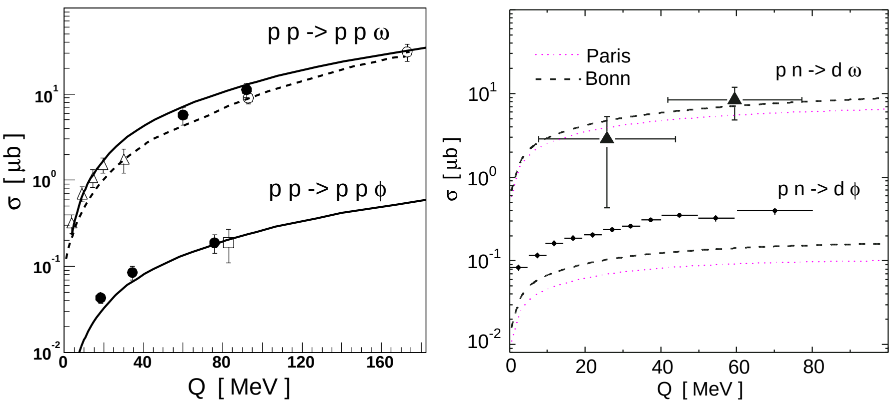

Figure 1: Excess-energy dependence of the total cross section in NN collision: Data points from SPESIII [4], DISTO [5] and COSY–TOF [6,16] in pp collisions are plotted as open triangles, a rectangle and circles, respectively. The data plotted as filled triangles and filled circles were obtained at ANKE [12–15]. Solid lines in the left panel as well as dashed and dotted lines in the right panel are taken from [19]. The dashed line in the left panel represents the dependence obtained by K.Nakayama *et al.* [20] without inclusion of nucleon resonances. See the text for further details.

However, the further extension of the experimental data set achieved during the last few years in experiments at COSY–TOF [16] and, especially, at ANKE [12–15] seems to change the scenario mentioned above. In particular, the total cross section of the $pn \to d\omega$ [12] has been measured to be almost a factor of 2 lower than any theoretical prediction [17, 18] available by that time. Taking into account these new data, L.Kaptari and B.Kämpfer [19] have achieved a good description of the $pp \to pp\omega$ cross section (solid line in Fig. 1) in the framework of the same model as in [7] but without involving any effects from nucleon resonances.

This discrepancy has been recently investigated by K.Nakayama *et al.* [20]. It was found that ω-production in NN collisions is more sensitive to the interference of nucleonic and mesonic currents than the $\pi^- p \rightarrow \omega n$ reaction which has been previously used for the determination of the relative sign between the $NN\omega$ and $\pi\rho\omega$ coupling constants. With the opposite sign compared to what has been used in earlier calculations [7], the energy dependence of the $pp \rightarrow pp\omega$ cross section presented in Fig. 1 by the dashed line was obtained in absence of resonances.

This analysis shows that the availability of accurate data for ω-production in the pn isospin channel is very important to establish the production mechanism. However, as one can see from the Fig. 1, the accuracy of existing data for the $pn \rightarrow d\omega$ reaction has to be significantly improved to make them really useful for this purpose. Furthermore, it is expected [17,19] that the angular differential cross section will provide an even more direct test of theoretical models than the total cross section which might be influenced by initial state interactions. A significant anisotropy of the angular distribution is predicted already at $Q \geq 60$–80 MeV (Fig. 2) but the existing data for the $pn \rightarrow d\phi$ reaction [14] have large uncertainties in this Q–range.

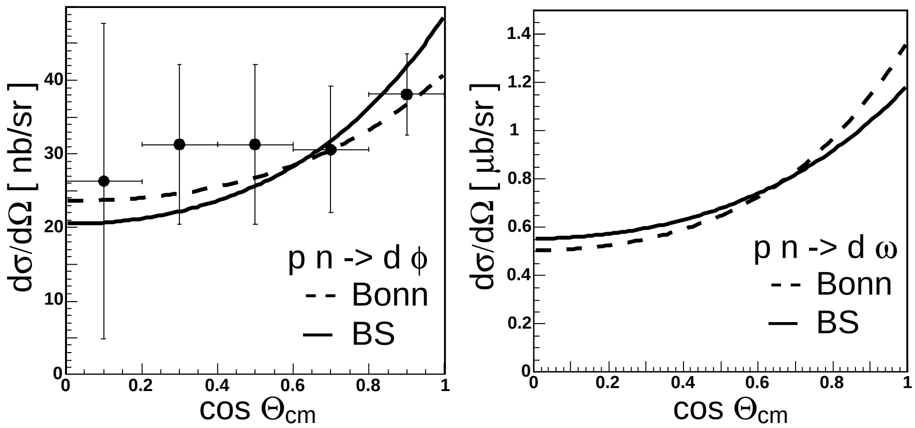

Figure 2: The differential cross section for the $pn \rightarrow d\phi$ at $Q = 80$ MeV (left panel) and for the $pn \rightarrow d\omega$ at $Q = 60$ MeV (right panel) predicted by L.Kaptari and B.Kämpfer in [19] using the Bonn potential (dashed lines) and the Bethe-Salpeter formalism (solid lines). In both cases the curves are normalized to the same total cross section. The black points represent experimental data from ANKE [14] measured at $< Q > = 70$ MeV. There are no experimental data for differential cross sections for the $pn \rightarrow d\omega$ reaction so far.

2.2 Test of the OZI Rule

It is well known (see e.g. [2, 21, 22]) that the ratio of the ϕ/ω yields (R) in hadronic interactions, when the initial and final hadrons do not contain strange quarks, is a particularly sensitive probe of the OZI rule [1] claiming that $s\bar{s}$ production is suppressed substantially. With the deviation $\delta = \theta - \theta_{\mathrm{i}} = 3.7°$

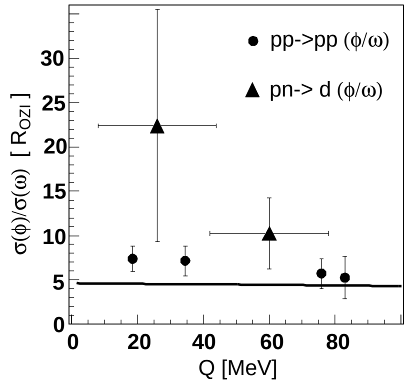

Figure 3: Ratio of the ϕ/ω total cross section expressed in R_{OZI} units as a function of excess energy. In the *pp* case (black circles) values are calculated using the approximation for the $pp \to pp\omega$ cross section from [15] and the $pp \to pp\phi$ cross section values from [5,13]. In the *pn* case (black triangles) data were taken from [12] and [14]. The solid line represents the prediction for the *pp* case obtained in [19].

from the ideal SU(3) mixing angle $\theta_{\mathrm{i}} = 35.3^\circ$ it leads to the value [2]

$$R_{OZI} = \tan^2(\theta - \theta_i) = 4.2 \cdot 10^{-3} = R/f,$$

where f is the ratio of phase-space factors.

However, experimental data show an apparent excess of R/f above this value which varies from $(10-30)\cdot 10^{-3}$ in πN and NN collisions to $(100-250)\cdot 10^{-3}$ in $\bar{p}p$ annihilation at rest and in flight. The origin of this enhancement is still unknown. In [22] the large excess of R in pp and $\bar{\mathrm{p}}$p collisions was interpreted in terms of “shake-out” and “rearrangement” of an intrinsic $\bar{\mathrm{s}}$s component in the nucleon wave function. On the other hand, in [23,24] the large excess in ϕ in $\bar{\mathrm{p}}$p annihilation at rest was explained in terms of hadronic intermediate $\mathrm{K}\bar{\mathrm{K}}^*$ states which might create ϕ mesons.

Furthermore, the combined analysis of the ϕ and ω production in *pp* interactions based on the meson–exchange approach [25,26] has found that the consistent description of the data from [5,6] does not require a large $NN\phi$ coupling constant but it is necessary to introduce a violation of the OZI rule at the $\pi\rho\phi$ vertex. This finding suggests an implicit enhancement of the ϕ/ω cross section ratio by a factor around 3 as compared to the R_{OZI} value. Moreover, as it was shown in [7,17,19], the dynamical effects due to the energy dependence of production amplitudes and their interferences may further increase the calculated ratio.

Therefore the experimental *pp* ratio seems to demonstrate a rather small excess over the model prediction (Fig. 3). On other hand, the data in the *pn* channel may indicate an energy dependence of the ϕ/ω cross section ratio while the theoretical ratio found in [19] is practically constant over the excess energy range.

3 Experimental Scheme

The part of the ANKE setup [27], which will be used to measure the $pd \to \mathrm{p_{sp}} d\omega$ reaction is shown in Fig. 4. The circulating proton beam interacts with the deuterium cluster-jet target placed inside the vacuum chamber in front of the ANKE spectrometer dipole. Two telescopes of a large–size position sensitive silicon detectors installed to the left and to the right side of the target inside the same vacuum chamber will identify spectator protons and reconstruct their three-momenta.

Deuterons from the reaction under investigation are emitted in forward direction. They will be detected in the forward detection system (Fd) of ANKE, consisting of three multi-wire proportional chambers (MWPCs), two layers of scintillators and 16 Čerenkov counters. The Fd system provides the three-momentum reconstruction and the particle identification.

The ω–meson production in the $pn \to d\omega$ reaction will be then identified using the missing–mass method as described in Section 4.

As compared with our first measurement [12], the main improvement of the proposed experiment comes from the use of new "spectator" detection system. The acceptance will be enlarged by about a factor 20, and an excess energy range up to 100 MeV will be covered with one beam momentum. Moreover, the acceptance gets more suitable for the determination of the angular differential cross section at Q >60 MeV (see Section 4). In addition, as described in Sections 3.2 and 3.3, this system allows a better energy determination of low momentum protons and a more reliable absolute normalization of the data.

It must be also noted that the efficiency of the Fd MWPCs has been significantly improved since the previous experiment.

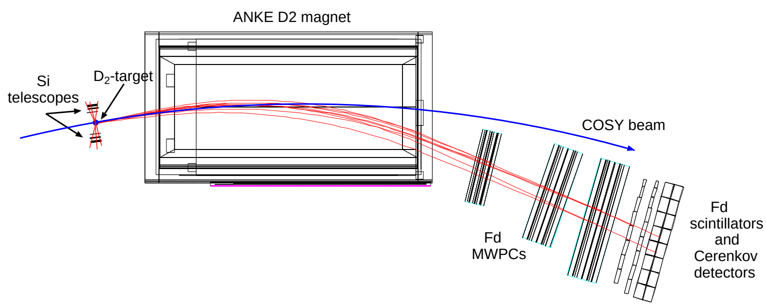

Figure 4: Part of the ANKE setup used for the measurements. Shown are the circulating COSY beam, the deuterium cluster-jet target and two telescopes of silicon detectors for spectator-proton detection. The ANKE spectrometer dipole D2 deflects forward going positively charged particles onto the forward detection system (Fd) used for the identification of fast deuterons and for the momentum reconstruction.

3.1 Fast Deuteron Identification

To study the proposed reaction close to threshold one has to distinguish fast deuterons with $\approx 2\,\mathrm{GeV/c}$ momentum from a 100 times larger proton background. To achieve this the following procedure has been developed and successfully used in our first experiment [12]. An optimal combination of ΔE-cut and proton-suppression factor providing a negligible loss of deuterons was found by simultaneous varying the ΔE-cut level and the Čerenkov-efficiency level. Using the chosen suppression factor, Fig. 5 shows projections along the energy-loss band of the deuterons ($\Delta E \propto \beta_{\mathrm{d}}^{-2}$) for the 2$^{\mathrm{nd}}$ hodoscope layer (dotted line). If one applies the energy-loss cut in the 1$^{\mathrm{st}}$ layer (solid line), the contribution of protons under the deuteron peak decreases below 10%. This can be seen, if one actively selects protons by a signal in the Čerenkov counters, and scales the distribution to the level of the background shoulder (dashed line).

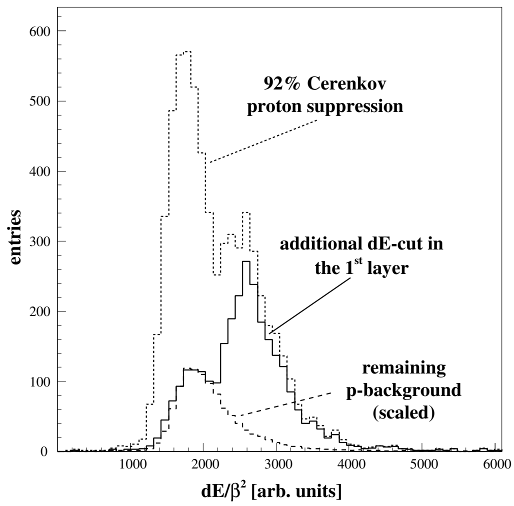

Figure 5: Energy loss in the 2$^{\mathrm{nd}}$ layer of the forward hodoscope scaled by $\beta_{\mathrm{d}}^{-2} \propto \Delta E(deuteron)$: Shown are distributions using Č-suppression only (dotted) and in addition using an energy-loss cut in the first layer (solid). The proton contribution has been extrapolated by an active selection of these particles and scaled accordingly (dashed).

3.2 Spectator Proton Detection

The determination of the excess energy in the quasi-free production requires not only the identification of the low energetic proton emitted from the deuterium target but also the reconstruction of its three-momentum. This can be achieved if the particle is detected in two position sensitive detectors possessing a good energy resolution as well. As the spectator proton momentum distribution has a maximum in vicinity of 50 MeV/c, the thickness of first detector, which the protons have to penetrate, should be chosen as small as possible. Each of Silicon Tracking Telescopes we plan to use in this experiment consists of three double–side segmented detectors.

- 1^{st} layer: 65 μm thick, 66.18×51.13 mm^2 active area, 316 strips with 210 μm pitch one one side and 256 strips with 200 μm pitch on the other side.

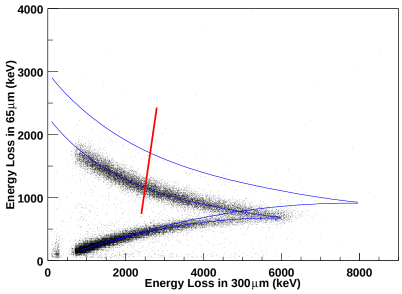

(a) $\Delta E 65\,\mu$m vs. $\Delta E 300\,\mu$m

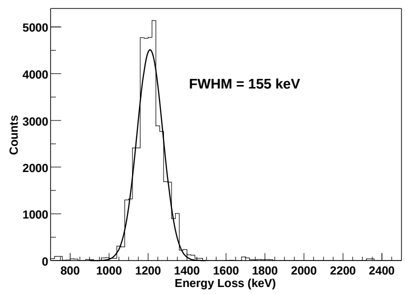

(b) energy resolution

Figure 6: The energy loss in the 65 μm versus the energy loss in the 300 μm thick detector shows only the proton-band, because it is situated under backward angles. In addition to the experimental data SRIM calculations for the energy losses of protons and deuterons are drawn. The projection on the indicated slice results in an energy resolution of about 160 keV FWHM.

- 2^{nd} layer: 300 μm thick, identical geometry compared with 1^{st} layer.

- 3^{nd} layer: 5000 μm thick, $64 \times 64\,\mathrm{mm}^2$ active area, 96 strips each side at a pitch of 666 μm.

By the use of the $\Delta E/E$-method for particle identification the energy range of the setup is naturally divided into two subsets. The first is the one where particles penetrate the 65 μm thick detector and are stopped in 300 μm silicon. This corresponds to proton kinetic energies of $2.5 - 6$ MeV. Protons penetrating the 300 μm detector and being stopped in the 5 mm thick detector [28] cover an energy range of $6.5 - 30$ MeV.

In view of the exponential behavior of the Fermi–motion momentum distribution above 50 MeV/c, the first and the second detectors deliver about 70% of total statistics. They have been parasitically tested during some experiment carried out at ANKE. Figure 6(a) shows the energy loss in the first 65 μm thin layer versus the energy loss in the second 300 μm thick layer under such experimental conditions when only protons could be detected. The obtained result well coincides with the calculated energy-loss proton band [29]. Furthermore the energy resolution along the slice which is indicated in figure 6(a) is determined to be $\approx$160 keV FWHM (fig. 6(b)). Thus the proton and deuteron band are expected to be separated by about $10\,\sigma$. Let us note that in our previous experiment proton and deuteron bands were separated only by about 2σ.

The capability of two-dimensional spacial resolution allows the full tracking of particles back to the target. Thus projections of the density distribution of the beam-target overlap can be produced easily in the detector plane. The principle and e.g. a distribution along the beam axis (z) is shown in Figure 7.

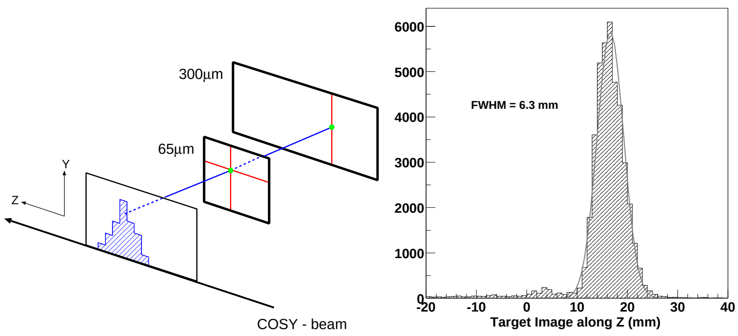

(a) projection of the target image (b) target extension along z

Figure 7: The target density distribution along the beam-axis

3.3 Absolute Normalization

The normalization of the data will be done using pd-elastic scattering [30, 31]. The third 5 mm thick detector is capable to stop elastically scattered deuterons with energies up to 40 MeV. They can be reliably separated from protons. The

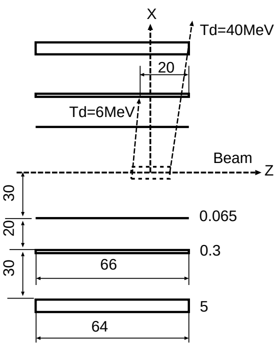

Figure 8: Arrangement of the two Silicon Tracking Telescopes (SPectator Left SPL and SPectator right SPR) within the ANKE target chamber (top view). In coincidence with the forward protons, deuterons from pd-elastic will be detected from $T_d = 6 - 40\,\mathrm{MeV}$ (all dimensions are given in millimeters).

forward 2 cm of the left-hand side spectator (SPL) telescope will be used to detect the deuterons from pd-elastic scattering over the full length of the target (see Figures 8 and 7) in coincidence with the fast protons in the Fd system. The measurement of the normalization reaction in the same detectors as the reaction under investigation minimizes a number of systematic uncertainties related to effects of the data–aquivision dead–time and of the efficiency of track reconstruction.

Furthermore, the self–triggering capability of the spectator system allows us to verify the alignment of all detectors in the Fd and in both the SPL and the right-hand side spectator (SPR) telescopes relatively to the center of target. In this case, with the simultaneous detection of pd elastic scattering in both the SPL and the SPR, their relative detection efficiencies will be kept under control as well.

4 Simulation Studies of $pn \to d\omega$

4.1 Acceptances

For a proton-beam momentum of 2.950 GeV/c events from the reaction $pd \to p_{sp}d\omega$ have been generated with help of the PLUTO program package which provides the Fermi-motion distribution inside the deuteron [32]. Figure 9 shows generated distributions for spectator protons and deuterons (all variables in the laboratory system). The ANKE acceptance limits for this reaction are indicated as shadowed regions. The restriction of the Fd momentum range from 1.5 to 2.7 GeV/c for forward going particles guarantees that more than 90% of the proton background from $pd \to p_{sp}pX$ reactions will be suppressed by Cerenkov counters (Section 3.1).

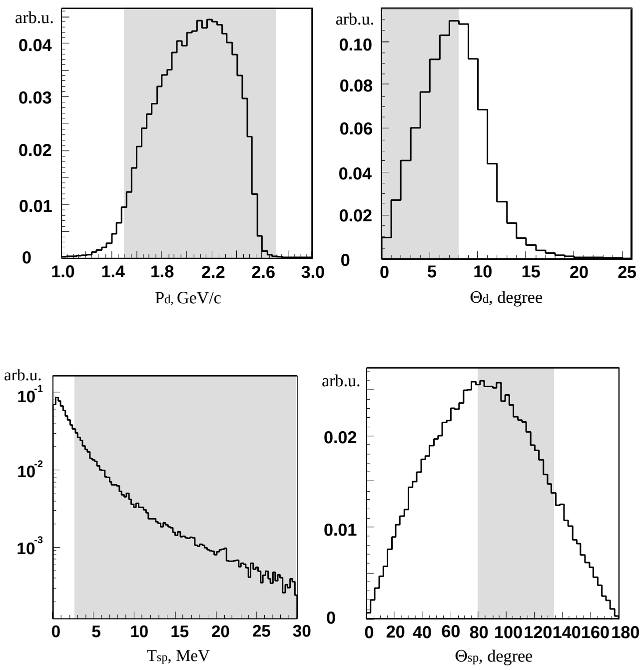

Figure 9: The spectator (T_{sp}, θ_{sp}) and deuteron (p_d, θ_d) distributions from $pd \to p_{sp}d\omega$ in the laboratory system. The shadowed regions indicate the ANKE acceptance limits.

These events have been traced using GEANT3 [33] through the ANKE detection system at a deflection angle of 6.9°.

Figure 10 shows the polar angle Θ_d^{cm} of the accepted deuterons in the pn center of mass system as a function of Q. The combined use of two spectator setups SPL and SPR allows to cover nearly all deuteron angles over the full Q-range.

To obtain an estimate how the total statistics of the experiment is distributed over the full Q-range, the experimental acceptance $\mathcal{A}(Q)$ and the $\sqrt{Q}$-weighted acceptance $\mathcal{A}_w(Q)$ have been calculated (see Figure 11). In the last case the

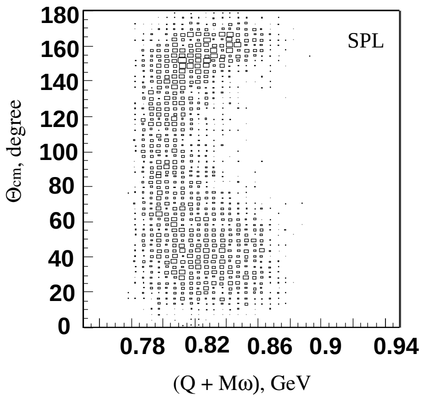

(a) Θ_d^{cm} vs. Q for deuterons in coincidence with SPL

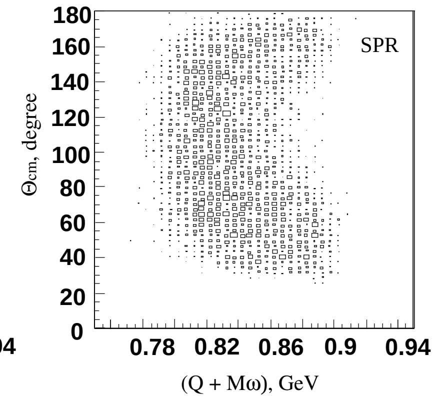

(b) Θ_d^{cm} vs. Q for deuterons in coincidence with SPR

Figure 10: The combination of SPL and SPR allows to cover nearly all Θ_d^{cm} of $pn \to d\omega$ in the pn center of mass system (The Q-range is shifted by the nominal value for the ω-mass of 781.9 MeV).

$\mathcal{A}_w$(Q)-distribution shows how the total statistics is distributed over the Q-range assuming phase space behavior of $\sigma_{tot}(pn \to d\omega) \sim \sqrt{Q}$.

Figure 12 shows the angular acceptance in a Q-range from 50-70 MeV over $\cos(\Theta_{cm})$.

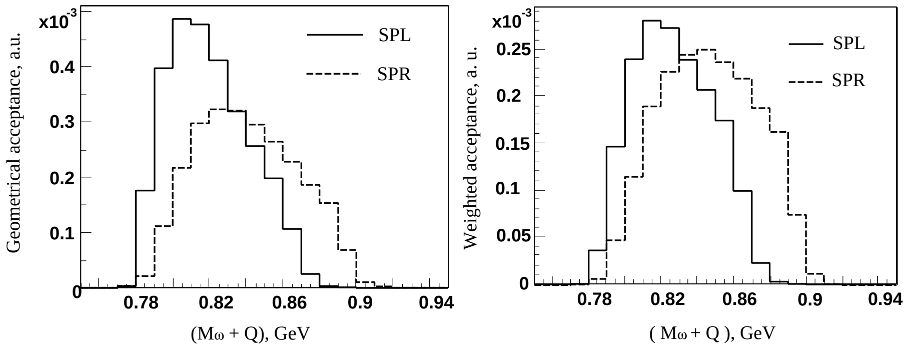

(a) acceptance $\mathcal{A}$(Q) (b) $\sqrt{Q}$-weighted acceptance $\mathcal{A}_w$(Q)

Figure 11: The experimental acceptance and the $\sqrt{Q}$-weighted acceptance are shown with a Q-binning of 10 MeV (The Q-range is shifted by the nominal value for the ω-mass of 781.9 MeV).

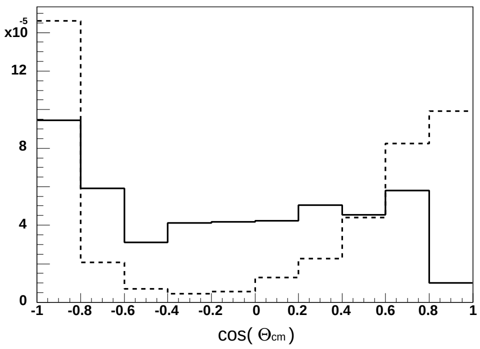

Figure 12: The angular acceptance in the Q-range from 50-70 MeV for SPL (dashed line) and SPR (solid line).

4.2 Missing-Mass Resolution for the ω-meson

The width of the reconstructed missing-mass of the ω has 4 main contributions (FWHM):

- 8 MeV from the natural width of the ω-meson.
- 7-8 MeV from the momentum and angular resolution of the reconstructed forward deuterons.
- 8-9 MeV from the energy and angular resolution of the reconstructed spectator protons.
- $\leq$ 2 MeV from the momentum resolution of the COSY beam which is assumed to be $\leq 10^{-3}$.

The individual contributions lead to the total missing-mass peak shown in Figure 13. Deuteron momenta have been smeared using $\sigma(\Delta p/p) = 1\%$, $\sigma(\Theta_{xz}) = 0.2°$ and $\sigma(\Theta_{yz}) = 0.1°$. These are already experimentally confirmed values for the reconstruction of the deuteron momenta. For the contribution of the spectator proton reconstruction small-angle scattering and track reconstruction in the silicon-strip detectors have been taken into account. This contribution together with the COSY-beam uncertainty leads to an experimental Q-resolution of $\Delta Q \leq 10$ MeV.

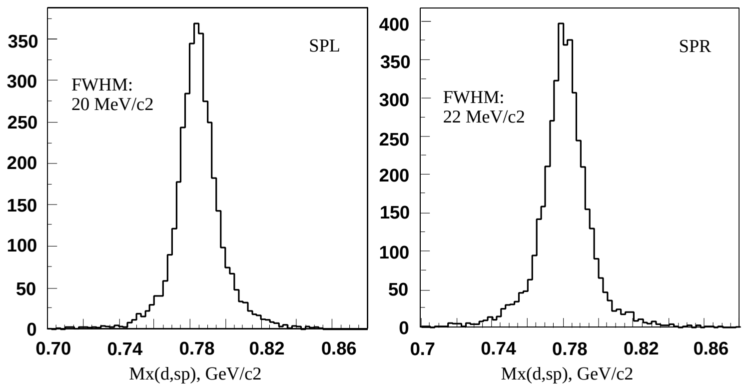

(a) In coincidence with SPL (b) In coincidence with SPR

Figure 13: Expected missing-mass distribution for the ω-meson.

4.3 Expected Missing-Mass Spectra

In the proposed study the ω-meson will be identified by the missing-mass method. To develop the strategy how to extract the ω-meson contribution out of the background, a full simulation of the missing mass-spectra has been performed. As it was found in our previous experiment [12], a quite reasonable description of the background can be achieved with a set of $pd \to (N \cdot \pi) dp_{sp}$ reactions ($N = 2..5$)

generated according the multi–particle phase space and convoluted with the ANKE acceptance. This was exploited here using the same parametrisation for the energy dependence of the total cross section. The phase space simulation of $pd \to \rho d p_{sp}$ and $pd \to \omega d p_{sp}$ reactions has been performed assuming the $\sqrt{Q}$ behavior of total cross section with the value of $\sigma_{tot} = 6\,\mu$b at Q=60 MeV.[1]

Figure 14 shows the resulting missing-mass spectra where contributions from all the simulated reactions were added with weights proportional to their cross sections.

In case of the SPL telescope, the ω–signal can directly be extracted as a peak above rather smooth background at $Q >$60 MeV. With the expected signal–to–background ratio $N_\omega/N_{bgd} \simeq 1/2.5$ we estimate that the collection of ∼3000 ω–events in the (60–80) MeV Q-range will provide a reference data of sufficient accuracy for the further consistent analysis of missing mass distributions measured with the SPR telescope.

Using the overlap of the SPL and SPR acceptances (Figures 11 and 12) the selection of the ω-signal from the background will be verified. Following this procedure we expect to achieve an accuracy of around 20% per $\cos\Theta_{cm} = 0.1$ angular bin in vicinity of $\Theta_{cm} = 90°$.

Together with the total cross section of 6 μb and the $\sqrt{Q}$ weighted acceptance of $\epsilon = 0.4 \cdot 10^{-3}$ (Fig. 11) this leads to a beam–time estimate of

$$T = 2.5 \cdot \frac{N_\omega}{\sigma \cdot L \cdot \epsilon} \approx 220\,h$$

A factor of 2.5 losses includes the data-acquisition dead-time and the efficiency of the track reconstruction in the the forward detection system. The track reconstruction efficiency in the Silicon Tracking Telescopes is assumed to be close to 1.

For lower Q-values we plan to determine the background shape under the ω–peak using the kinematical transformation of missing mass spectra measured within different excess energy ranges. This method has been successfully applied in earlier experiments at ANKE [12, 15].

[1]Although in the previous experiment $\sigma_{tot} = 9\,\mu$b has been determined at $< Q >= 60$ MeV, in view of large uncertainty of the result we prefer to use a more conservative estimate. Moreover, with the predicted anisotropic angular distribution (see section 2) the value 9 μb should be corrected to the value of 7.6 μb.

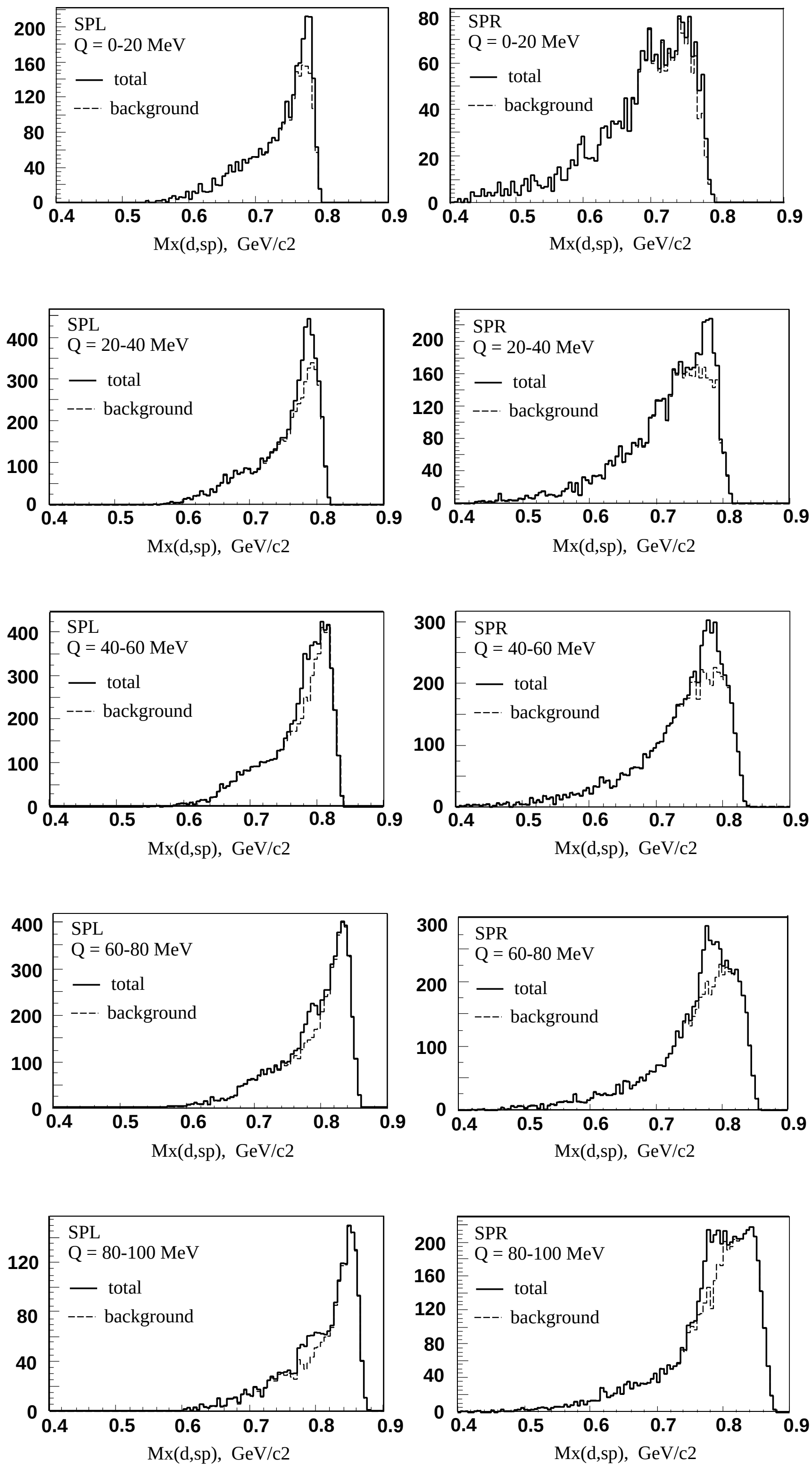

Figure 14: The missing-mass spectra from Q=0-100 MeV with a binning of 20 MeV.

5 Requested Time For Measurements

We request **two weeks** of beam-time to study the $pn \to d\omega$ reaction with the aim to extract the total and differential cross-section over the excess energy range from 20 MeV to 100 MeV with the Q–binning of 10–20 MeV. Using the new detection system for measuring of spectator protons and our experience obtained in previous experiments on the ω–meson production at ANKE [12, 15] we plan to improve the accuracy of the measurement by a factor of 4–5 as compared with the existing data.

References

[1] S. Okubo, Phys. Lett. B **5** 165 (1963).
G. Zweig, CERN Report **8419/TH 412** (1964).
I. Iizuka, Prog. Theor. Phys. Suppl. **37–38** 21 (1966).

[2] H.J. Lipkin, Phys. Lett. B **60** 371 (1976).

[3] C.Hanhart, Phys.Rep. **397** 155 (2004).

[4] F.Hibou et al., Phys. Rev. Lett. **83** 492 (1999).

[5] F.Balestra et al., Phys.Rev. C **63**, 024004 (2001).

[6] S.Abdel-Samad et al., Phys.Lett. B **522**, 16 (2001).

[7] K.Tsushima, K.Nakayama, Phys.Rev. C **68**, 034612 (2003).

[8] C.Fuchs et al., Phys.Rev. C **67**, 025202 (2003).

[9] A.Faessler et al., Phys.Rev. C **70**, 035211 (2004)

[10] G.Penner, U.Mosel, Phys.Rev. C **65**, 055202 (2002); arXiv:nucl-th/0207066.

[11] A.I.Titov, T.–S.H.Lee, Phys.Rev. C **66**, 015204 (2002);

[12] S.Barsov et.al., EPJ A **21**, 521 (2004).

[13] M.Hartmann et al, Phys.Rev.Lett. **96**, 242301 (2006).

[14] Y.Maeda et al., Phys.Rev.Lett. **97**, 142301 (2006).

[15] S.Barsov et al., Eur.Phys.J. A **31**, 95 (2007).

[16] M.Abdel-Bary et al., arXiv:nucl-ex/0702059 (2007).

[17] K.Nakayama, J.Haidenbauer, J.Speth, Phys. Rev. C **63**, 015201 (2000).

[18] V.Grishina et al. Phys.Atom.Nucl. **63** 1824 (2000).

[19] L.P.Kaptari, B.Kämpfer, Eur.Phys.J. A **23**, 291 (2005).

[20] K.Nakayama et al., arXiv:nucl-th/0611101 (2006).

[21] J.Ellis, E.Gabathuler and M.Karliner, Phys.Lett. B **217**, 173 (1989).

[22] J.Ellis, M.Karliner, D.E.Kharzeev and M.G.Sapozhnikov, Phys.Lett. B **353**, 319 (1995).

[23] M.P.Locher, Y.Lu and B.S.Zou, Z.Phys. A **347**, 281 (1994).

[24] D.Buzatu and F.Lev, Phys.Lett. B **329**, 143 (1994).

[25] K.Nakayama, A.Szczurek, C.Hanhart, J.Haidenbauer and J.Speth, Phys.Rev. C **57**, 1580 (1998).

[26] K.Nakayama, J.W.Durso, C.Hanhart, J.Haidenbauer and J.Speth, Phys.Rev. C **60**, 055209 (1999).

[27] S.Barsov et al., Nucl.Instr.Meth. A **462 (3)**, 364 (2001).

[28] G. Riepe, D. Protic, Nucl.Instr.Meth., **226**, 103 (1984).

[29] SRIM, The Stopping and Range of Ions in Matter, version 2000.24, http://www.srim.org

[30] S. Barsov et al., *Luminosity Determination at ANKE with the Spectator Detector*, Annual Report of the IKP 1999, p. 21

[31] Yu. Uzikov, *Diffraction pd-scattering at COSY energies*, Annual Report of the IKP 2001, http://www.kfa-juelich.de/ikp/publications/AR2001/CHAP1/mpddiff_yuri.pdf

[32] http://www-hades.gsi.de/computing/pluto.html/PlutoIndex.html

[33] CERN Program Library W5013, CERN, 1993; http://wwwinfo.cern.asdoc/geant$_h tml3/geantall.html$